RESEARCH ARTICLE

BULLETIN OF SCIENTIFIC RESEARCH

Asian Research Association

DOI: 10.54392/bsr2521

Influence of the Presence of Aluminum and of its Content on the As–Cast Microstructure of Alloys Designed to be Tac–Reinforced

Patrice Berthod [1, *]

[1] Department Institut Jean Lamour, Université de Lorraine, Nancy, 54000, France.
*Corresponding author Email: patrice.berthod@univ-lorraine.fr
DOI: https://doi.org/10.54392/bsr2551
Received: 06-09-2025; Revised: 26-11-2025; Accepted: 05-12-2025; Published: 14-12-2025

Abstract: Four alloys based on either cobalt or nickel, containing tantalum and carbon for creep–resistance purpose (based on TaC carbides), as well two aluminum contents for hot oxidation–resistance purpose (alumina–forming behavior), were conventionally cast. Their microstructures in the as–cast conditions were characterized. As expected, all alloys contain a dendritic matrix and TaC as single carbide type present. However, differences were noticed among the four alloys concerning the distribution of the TaC carbides. As expected, in the two alloys containing 5 wt. % Al, Co-based or Ni-base, the tantalum carbides were successfully obtained as an interdendritic network of eutectic script TaC carbides. This was more or less different for the {10 wt. % Al}–containing alloys for which the TaC phase crystallized according to two successive liquid–solid transformations. Obviously, for the two former alloys, TaC appeared first as pre–eutectic particles, and second, after the dendritic development of the matrix, as eutectic script carbides. The cobalt alloy contained a majority of interdendritic eutectic script TaC and a minority of blocky pre–eutectic TaC segregated to the periphery of the ingot. The carbides distribution in the nickel alloy was inversed, with the greatest part of TaC carbides formed prior to the matrix crystallization and massively segregated in the outermost part of the ingot. The high temperature properties of this last alloy were controlled at 1200°C and this showed that, in addition to the good oxidation behavior, the {10 wt.% Al}–containing nickel alloy demonstrated nevertheless a correct creep–resistance.

Keywords: Cast Co and Ni alloys, Tantalum Monocarbides, Aluminum, Metallographic Characterization, High Temperature Oxidation, Creep–Resistance

1. Introduction

The alloys strengthened by carbides, which represented an important family of superalloys several decades ago [1], are still today of high interest. Indeed, they can be creep–resistant independently of gamma prime precipitates, thanks to other strengthening particles staying in the microstructure up temperatures above 1100°C. Chromium carbides are efficient in this role below 1000°C while more heat–resistant carbides are able to maintain the mechanical resistance at higher temperatures at which the gamma prime partially or totally dissolve [2]. This is the case of the tantalum monocarbides which are persistent at 1200°C and even several tens of °C higher, although they know morphology evolution possibly causing a decrease in their reinforcing effect [3-5]. These carbides are exploited in a long series of industrial superalloys, base on cobalt (e.g. [6, 7] or nickel (e.g. [8, 9]) for the help that they bring to the resistance against mechanical deformation and rupture at elevated temperatures. Generally, TaC are present in the microstructures of superalloys in co-existence with other carbides. In the early beginning of the 2000's years reinforcing carbine networks made of TaC exclusively started to be extensively explored in chromium–rich cobalt – based (e.g. [3,4]) and nickel–based (e.g. [10]) superalloys, and in Cantor–based high entropy alloys [11,12].

Many of these alloys based their chemical resistance at high temperature on chromium, by containing around 30 wt.% of this element. Indeed, with such contents, Cr allows the alloys developing an external continuous Cr2O3 scale by selective oxidation of Cr [13, 14]. This chromia scale protect the alloys against further oxidation thanks to its obstruction to the cationic and anionic diffusion. The protection against both oxidation by gases and corrosion by melts that chromia brings at high temperature is a little limited by several problems: 1/ chromia is not really a stoichiometric oxide (while alumina is [13,14]) and thus not very efficient to slow down ionic diffusion, 2/ it can be re-oxidized to give gaseous specie CrO3 [15] (phenomenon not possible for alumina), 3/ the

presence of chromium in high quantity in the bulk of the alloy may threaten the 100% TaC network (Cr is also an efficient carbide–forming element, Al does not), notably for nickel–based alloys [10].

For uses above 1100°C, retaining an efficient mechanical reinforcement by keeping TaC carbides and taking benefit from the efficiency of alumina to resist oxidation is may be possible with superalloys containing both Ta & C and Al in contents high enough. Exploring this possibility led us to design the TaC–strengthened alumina forming cobalt–based and nickel–based elaborated in this work and whose as–cast microstructures will be investigated here.

2. Materials and Methods

2.1 Preparation of the Alloys for the Study

A total of four alloys, two based on cobalt and two based on nickel, were synthesized by induction foundry under inert atmosphere. The targeted compositions were: Co(bal.)-0.4C-6Ta-5Al (wt.%, "Co5" alloy), Co(bal.)-0.4C-6Ta-10Al ("Co10"), Ni(bal.)-0.4C-6Ta-5Al ("Ni5"), and Ni(bal.)-0.4C-6Ta-10Al ("Ni10").

The used furnace was a CELES high frequency induction (Figure 1a), composed of 1/ a copper crucible which is continuously cooled by internal circulation of fresh water, 2/ a silica tube closing the melting chamber, 3/ a coil surrounding the tube at the same height as the crucible which was itself internally water–cooled when the high frequency alternative current (several Amperes, about 100 kHz and 5 kV) was applied by the HF generator. When the combustion was open, the parts of pure elements (Alfa Aesar, purity > 99.9%) were put and mixed in the crucible. After chamber closing, primary vacuum was achieves three times, alternating with the introduction of pure argon. Just before heating start, the internal atmosphere was composed of 500 mbars of Ar.

2.2 Metallography and Composition Control

Each of the four ingots was cut to obtain a part for metallographic examination of the as–cast microstructures and the control of the obtained chemical composition (Figure 1b). Each was embedded in a resin mixture rigidifying at room temperature and ground (SiC papers from #240 to #1200) then polished (textile disk enriched with hard micrometric particles). The obtained mirror–like samples were observed to control their microstructure, using a Scanning Electron Microscope (SEM JEOL JSM6010LA) using the Back Scattered Electrons imaging mode (BSE) (Figure 1c). Their chemical compositions were measured using the Energy Dispersion Spectrometry apparatus of the SEM (EDS).

2.3 Additional Tests

As this will be seen farther, the as–cast Ni10 alloy presents a very particular microstructure, very different from the three other studied alloys. To discover the consequences of its particular microstructure it has been subjected to an oxidation test (50h at 1200°C in air) and to a creep–test (15 MPa tensile stress generated by 3 point bending, 1200°C, 100h). For the oxidation test a parallelepiped with the following approximate dimensions – 10 mm × 10 mm × 3 mm – was cut and ground all around with #1200 SiC paper. For the creep test, this is another parallelepiped, with these other following approximate dimensions – 15 mm (length) × 2 mm (width) × 1 mm (thickness) – which was prepared.

3. Results and Discussion

3.1 Microstructures in the As–Cast Condition

The microstructures of the two alloys containing 5 wt.% Al after their elaboration are presented in Figure 2 a and b (for the "Co5" alloy) and in Figure 3 a and b ("Ni5"), by low and high electron micrographs taken with the scanning electron microscope in the back scattered electrons mode.

The "Co5" alloy is mainly made of a grey dendritic matrix (Co–based solution of about 4 wt.% Al and 2 wt.% Ta) and a dense interdendritic eutectic compound involving matrix and script particles of a bright phase. Some rare blocky particles of this same bright phase are present too. These coarse ones, thanks to their compact shape and their size, allowed identifying this phase which is TaC (about 50 at.% Ta and 50 at.% C).

The matrix of the "Ni5" alloy is also dendritic and this Ni–base solid solution also contains Al and Ta, in quantities higher than in the "Co5" alloy's one: about 5 wt.% Al and 5 wt.% Ta here. The "Ni5" alloy also contains an interdendritic network of a eutectic mixture of matrix and script TaC carbides much less dense than the "Co5" one. The part of matrix taking part to the eutectic compound is darker than the pre–eutectic one due to a lower content in tantalum (3 wt.% Ta only, for the same 5 wt.% Al).

With 5 wt.% Al more, these two alloys become very different. Effectively, the "Co10" alloy presents a matrix – dendritic again – but now double–phased (Figure 4 a and b). Its matrix is made of a grey one – containing about 7 wt. % Al and 2 wt. % Ta – and a much darker one which contains almost the same quantity of Ta but the double quantity of aluminium (13 wt. % Al). By considering the atomic composition of this dark part of the matrix, it appears that it is probably the Co_3Al intermetallic compound.

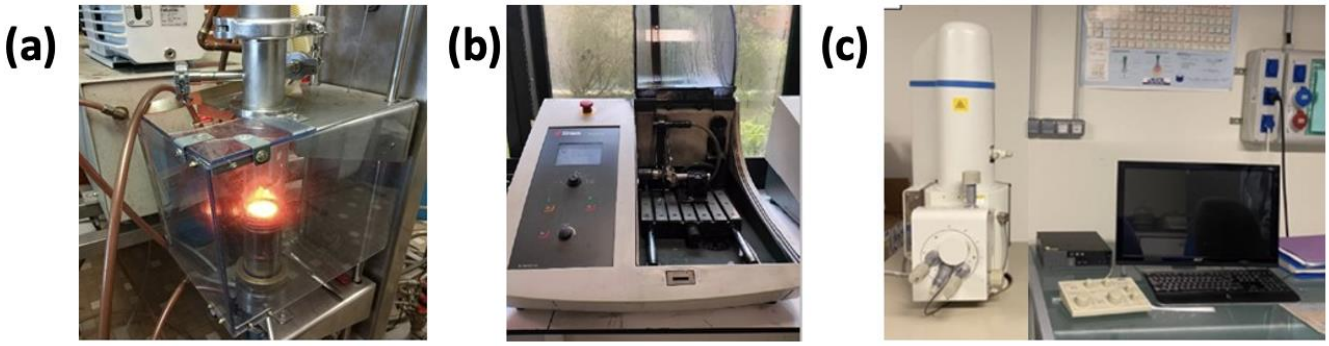

Figure 1. Some of the used experimental equipment (a) the elaboration furnace, (b) the precision saw, (c) the SEM.

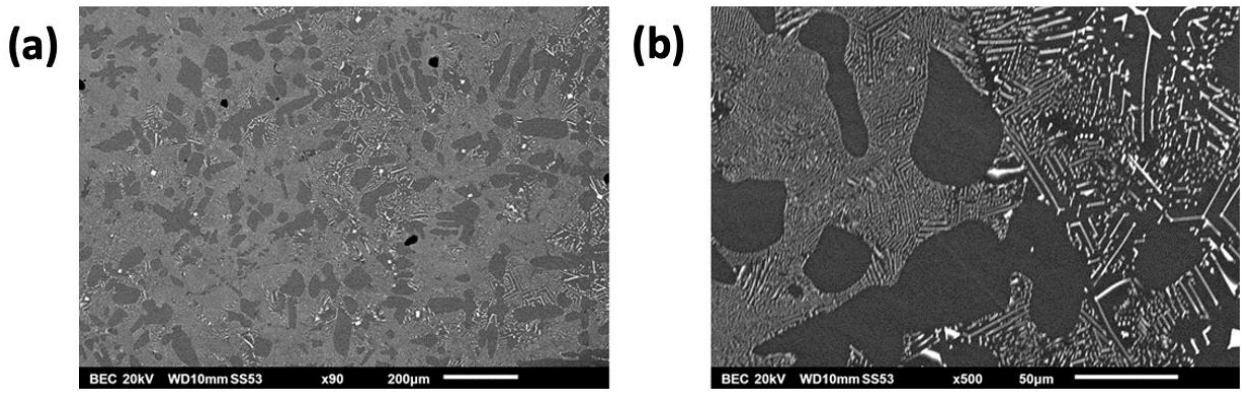

Figure 2. Low (a) and high (b) magnification SEM/BSE micrographs of the “Co5” microstructure.

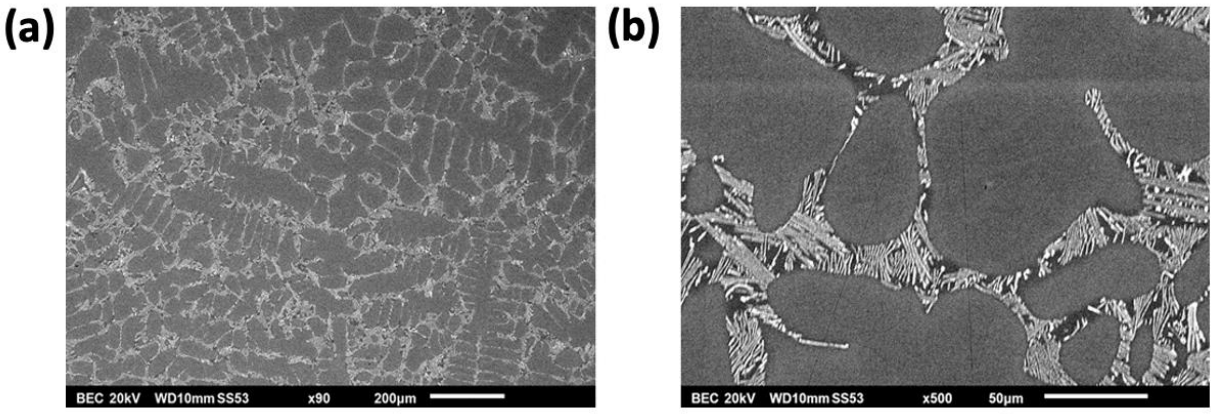

Figure 3. Low (a) and high (b) magnification SEM/BSE micrographs of the “Ni5” microstructure.

The population of TaC carbides is obviously itself double: an interdendritic network of eutectic script tantalum carbides which seems to be significantly less dense than in the “Co5” alloy although they both contain the same quantity of tantalum, and some coarse blocky TaC.

The microstructure of the “Ni10” alloy is totally different from the ones of the three first alloys (Figure 5 a and b). Indeed, it seems totally free from interdendritic eutectic script TaC carbides and the TaC phase is represented only by some dispersed blocky particles. The matrix (which contains about 9 wt.% Al and 3 wt.% Ta, average values), represents almost the whole alloy. It seems chemically heterogenous (zones more or less dark).

The chemical compositions of all alloys were checked by using the Energy Dispersion Spectrometer equipping the SEM. Their Ta and Al contents are the following values:

- Co5: 4.1 Al – 7.9 Ta (wt.%)
- Ni5: 4.6 Al – 7.5 Ta (wt.%)
- Co10: 8.8 Al – 5.3 Ta (wt.%)
- Ni10: 8.7 Al – 3.9 Ta (wt.%)

Due to a limited loss of Al – very oxidable element – by oxidation with the traces of oxygen existing in the commercial argon, all contents in Al seems normal. The Ta contents higher than the targeted 6 wt.% are due to the usual overestimation induced by the high exposure to the electrons beam and to the spectrometer of the tantalum carbides in relief after mirror polishing. In contrast the low and very low Ta contents in the Co10 and Ni10 alloys are surprising.

This become easily explainable when one have a look to the bottom to the two corresponding ingots: there are here, in both cases, an accumulation of very coarse TaC particles took place during solidification. This phenomenon did not occur for the "Co5" and "Ni5" alloys (Figure 6) but it was very important for the "Co10" and "Ni"10" alloys (Figure 7). This can be interpreted as the consequence of a pre–eutectic crystallization of TaC carbides just before the start of nucleation and growth of the dendritic matrix. These TaC particles, certainly heavier than the liquid (they are particularly rich in tantalum), moved downwards and accumulate in the lowest part of the liquid. This impoverished in Ta and in C the solidifying liquid and, at the end of solidification, the greatest part of the ingot contains less TaC than expected. This lack of TaC phase is visible in the core of the "Co10" ingot (TaC volume fraction significantly lower than the "Co5" and even "Ni5" alloys) and spectacular in the core of the "Ni10" alloys in which only some dispersed blocky TaC are visible. An additional explanation for the presence of less TaC in "Co5" than in "Ni5", and in "Co10" than in "Ni10", is the fact that the Ni–base matrix contains more Ta (between 3 and 5 wt.%) than the Co–base matrix (2 wt.%Ta). This should be the same for carbon but this too light element is not measurable (except in the blocky TaC carbides in which it is highly present). Such behaviour was not noticed in the Co-30Cr-0.4C-6Ta and Ni-30Cr-0.4C-6Ta (wt.%) alloys elaborated following the same procedure in the last decades. Obviously, the presence of aluminium (particularly with a 10 wt.% content), changed the successive steps of solidification, leading to the formation of many TaC which cannot be exploited by the alloys for their high temperature mechanical properties while elaborating such alloys is costly (Ta is an expensive element).

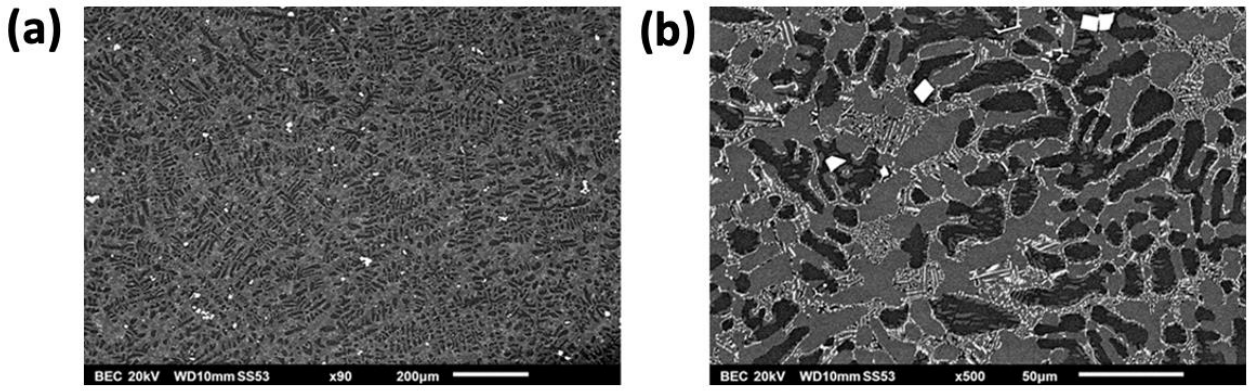

Figure 4. Low (a) and high (b) magnification SEM/BSE micrographs of the "Co10" microstructure.

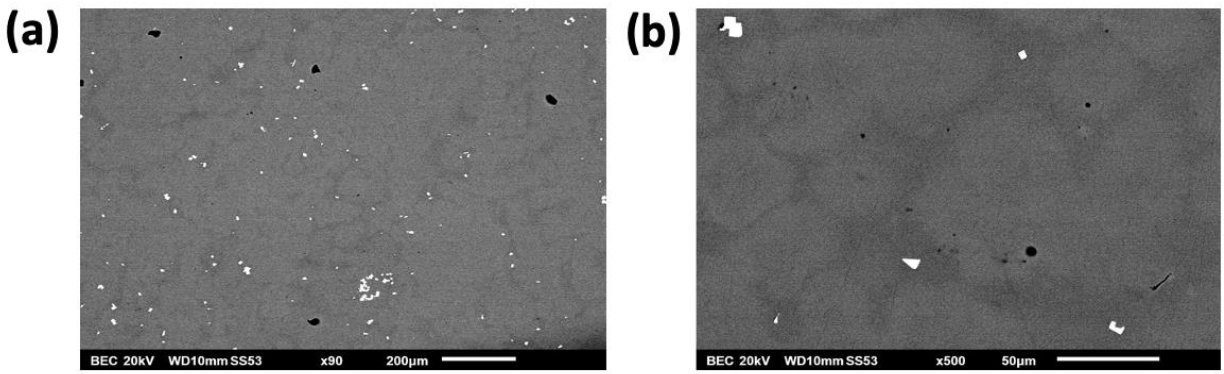

Figure 5. Low (a) and high (b) magnification SEM/BSE micrographs of the "Ni10" microstructure.

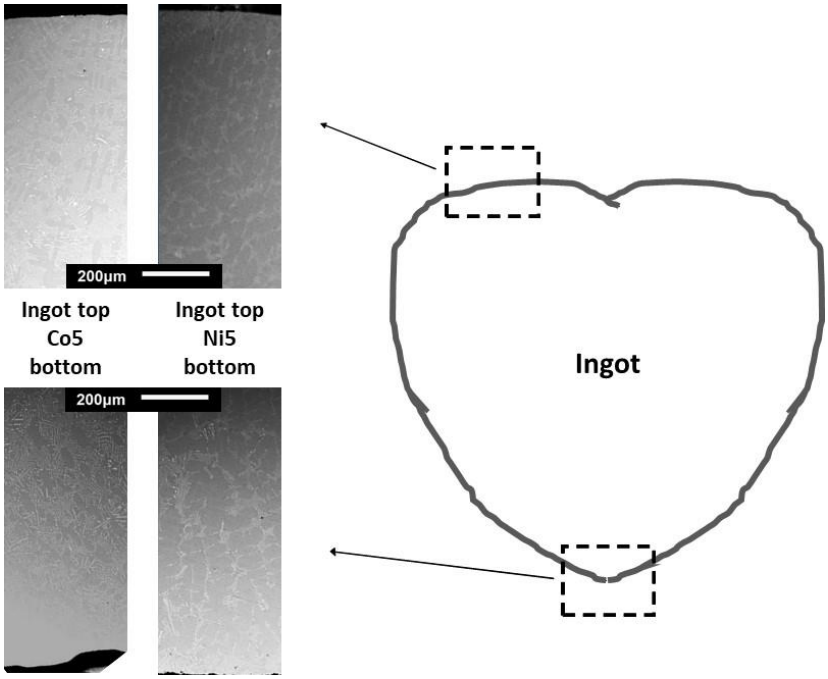

Figure 6. Absence of TaC accumulation in the bottom parts of the “Co5” and “Ni5” ingots.

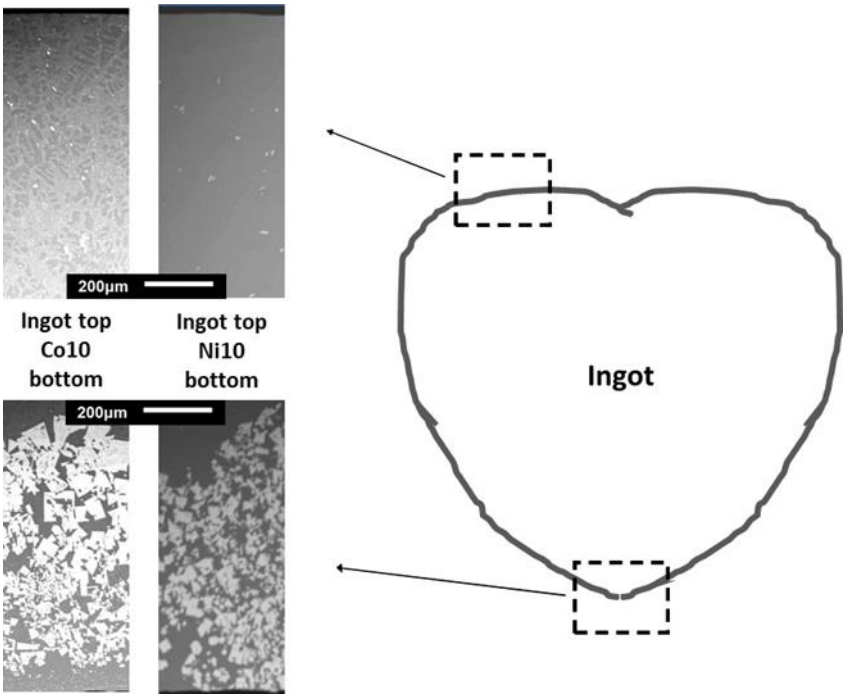

Figure 7. Important TaC accumulations in the bottom parts of the “Co10” and “Ni10” ingots.

This is thus to be avoided. It will be interesting to observe how new Al–rich Co–base and Ni–base alloys with lower contents in Ta and C will behave during their solidification, in order to verify whether TaC–reinforced alumina–forming alloys is really a metallurgical principle of interest.

3.2 High Temperature Properties of the “Ni10” Alloy

The properties in hot oxidation and hot corrosion by melts, as well as the thermomechanical properties such as thermal expansion or resistance to tensile stress and to creep, of the “Co5”, “Ni5” and even “Co10” alloys – which all present potentially interesting microstructures – will be extensively studied in the near future. In the present work, there are only some high temperature properties of the “Ni10” alloy, which were explored by a limited number of tests, in order to check whether it can be able to demonstrate interesting behavior despite its microstructure very poor in tantalum carbides.

The “Ni10” alloy was first subjected to oxidation at 1200°C for 50 hours in air using a thermobalance. The obtained mass gain curve was parabolic and

shows a rather slow oxidation kinetic (Figure 8a), suggesting that an external oxide layer developed all around the sample and protected the alloy. After extraction out of the thermobalance a major part of this oxide scale was lost, either during the cooling or during handling (Figure 8b and c, optical and electron microscopies).

Plotting mass gain versus the square root of time led to an approximatively straight line, the slope of which allowed specifying the parabolic constant Kp involved in the $\Delta m/S = (2 \times Kp)^{1/2} \times t^{1/2}$ formula describing the mass gain curve ($\Delta m/S$: mass gain per surface unit area, t: time). The obtained value, $Kp \cong 20 \times 10^{-12}$ g^2 cm^{-4} s^{-1} is about three times lower than for similar alloys containing 30 wt.%Cr instead 10 wt.% aluminum.

By considering the mass variations recorded during the heating before the 50 hours stage at 1200°C, and during the cooling at the end of this same isothermal stage, it appears that oxidation started early to be detectable by the thermobalance (when temperature reached about 500°C), as shown in Figure 9a. The second graph of Figure 9b shows the mass variation all along the whole thermal cycle and one can see that mass started decreasing as soon as temperature went above about 700°C. The mass loss is important, which suggests that the loss of the external oxide occurred mainly by oxide scale spallation during the cooling. In contrast with the interesting slow isothermal mass gain, this low adherence of the oxide scale on the cooling alloy indicates that, in its present state, this alloy is not suitable for service involving thermal cycles.

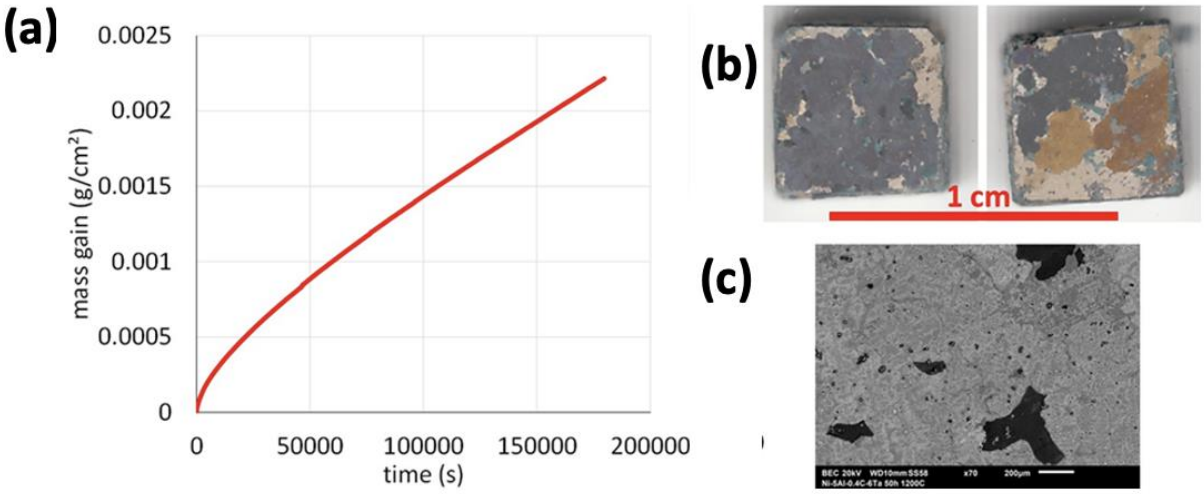

Figure 8. (a) The recorded mass gain plotted versus time and (b) surface states of the oxidized “Ni10” samples (optical macrographs on both main sides) and (c) SEM/BSE micrograph.

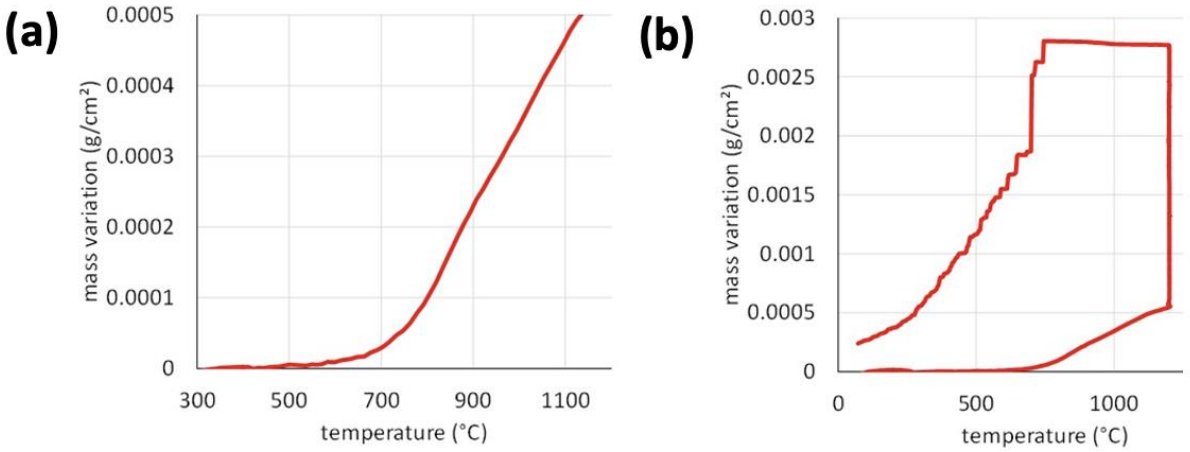

Figure 9. Enlargement of the {mass variation versus temperature} curve on the heating part (a) and general view of the whole thermal cycle (b) to also observe the mass behavior during cooling (oxide scale spallation).

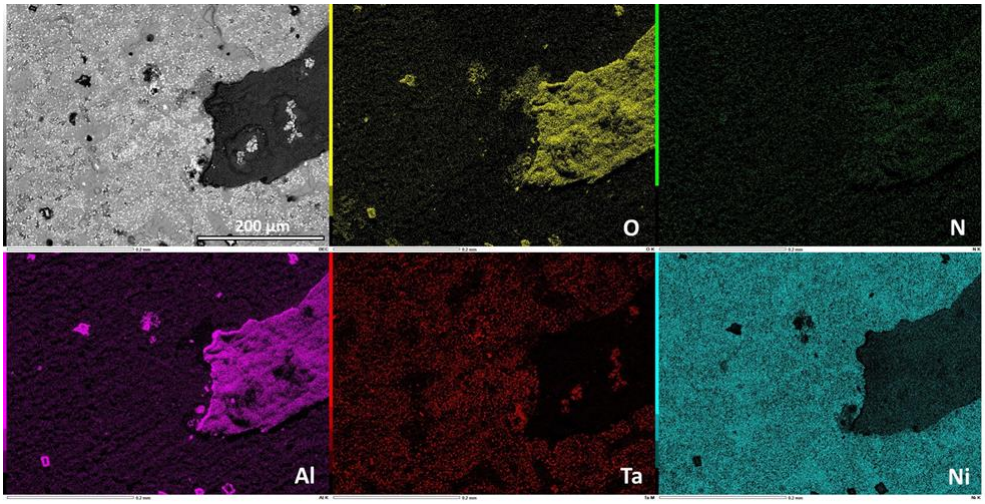

Figure 10. Elemental EDS mapping of the surface of the sample oxidized for 50 hours at 1200°C.

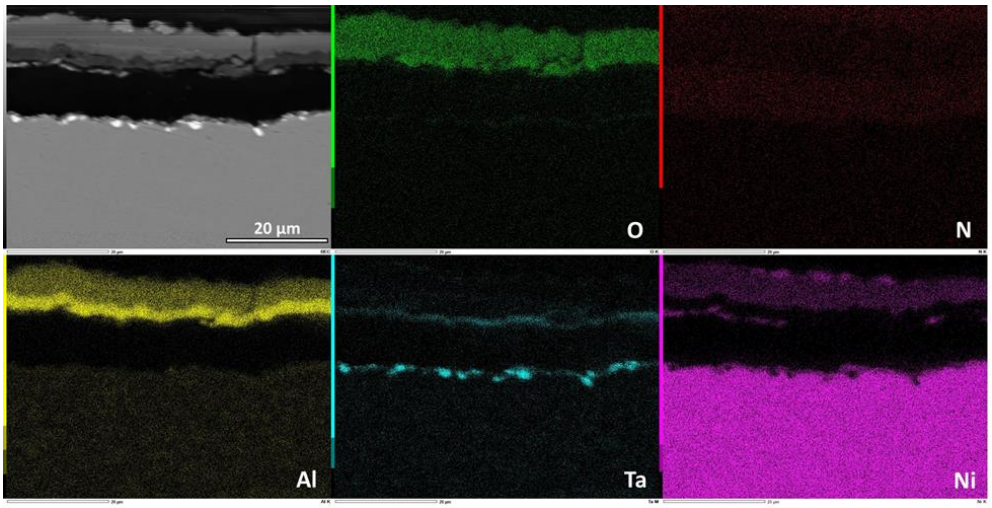

Figure 11. Elemental EDS mapping of the external oxide and of the subsurface of the sample oxidized for 50 hours at 1200°C.

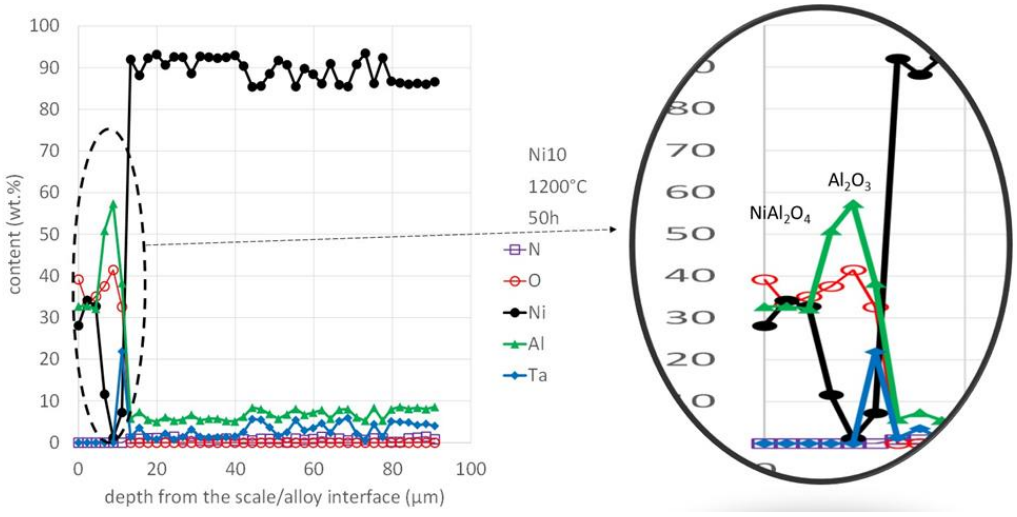

Figure 12. EDS concentration profiles acquired through a part of the external oxide scale and in the subsurface of the sample oxidized for 50 hours at 1200°C.

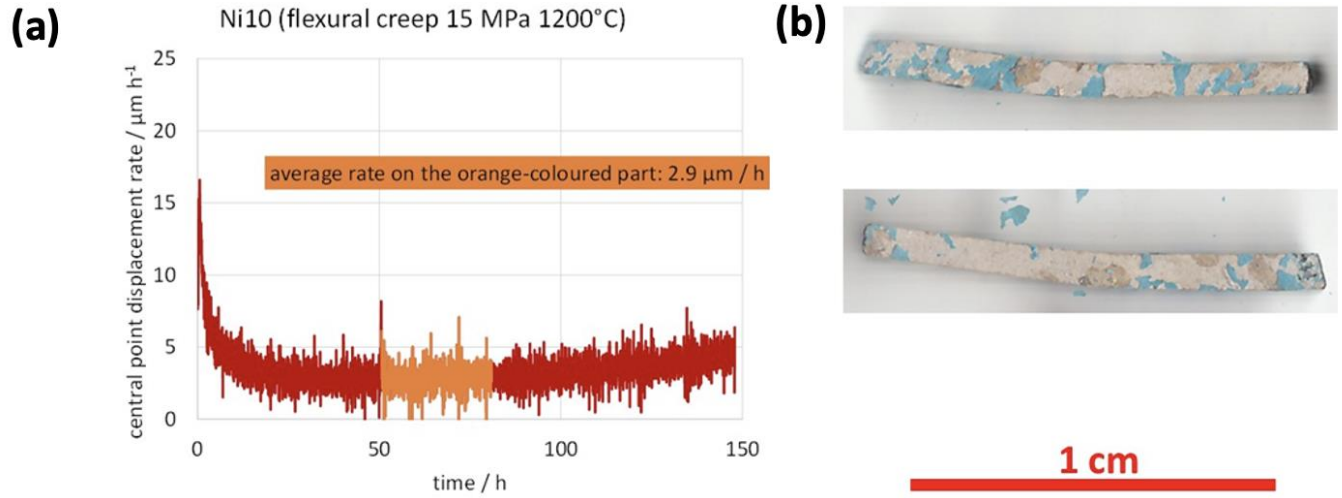

Figure 13. (a) Deformation curve of the parallelepiped sample for 15 MPa (central bottom part of the parallelepiped) at 1200 °C and (b) macrographs of the two sides of the crept sample.

The SEM/BSE micrograph and the elemental cartography presented in Figure 10 show that the rare parts of external oxide remaining on the surface of the sample are aluminum oxide with a possible participation of nickel. One can also notice the presence of tantalum but seemingly not with oxygen. The equivalent acquisition achieved on the oxidized and subsurface parts of the sample in cross–section presented in Figure 11, as well as the concentration EDS profiles plotted in Figure 12 across the oxide and the subsurface affected by oxidation, are more informative: the external scale was a superposition of the $NiAl_2O_4$ spinel (outermost location) and alumina (Al_2O_3, innermost). Both are protective oxides, particularly alumina, which explains the slow mass gain by oxidation for the elevated test temperature (1200°C). By considering the very limited Al–impoverishment in subsurface (concentration gradient very slightly tilted, almost horizontal), one can imagine that the alloy was possibly able to resist oxidation much longer. The resistance of the “Ni10” alloy against creep has also been controlled. The centered three-point flexural test at 1200 °C with a constant load calculated to produce a local tensile stress equal to 15 MPa was performed during 150 hours (Figure 13 a and b). After a rather short fast but decelerating deformation phase the downwards movement of the upper central point was uniform with a displacement rate of only 2.9 µm per hour. It is true that slighter-acceleration after 100 hours can be noticed, but the it seems that, despite the lack of TaC carbides (migrated to the bottom of the ingot), the creep resistance at 1200°C of this alloy is of interest. One can guess that it can be slowed down again if one succeeds to maintain TaC carbides in the center of the ingot.

4. Summary and Conclusion

Substituting chromium by aluminum for the hot oxidation resistance of these Co–based and Ni–based alloys containing the same Ta and C contents to obtained a TaC network for their high temperature creep resistance led to microstructures quite different from the ones of the initial {Co or Ni}–30Cr–0.4C–6Ta (wt.%) alloys studied earlier. Removing the carbide–former element chromium allowed obtaining TaC as single carbide phase while this was not the case for the nickel alloys in which chromium carbides formed at the expense of tantalum carbides (in contrast with the cobalt alloys for which TaC privileged). Due to the {30Cr by 5Al, wt.%}–replacement the interdendritic network of script eutectic TaC of the cobalt alloy becomes much denser while the interdendritic network of eutectic carbides is successfully made of TaC carbides exclusively. With 5 wt.% Al more, the matrix of the cobalt alloy becomes double–phased, composed – in equivalent volume fractions – of the Co–based solid solution and of the Co_3Al intermetallic, while a part of the formed TaC is of a pre–eutectic nature and segregates as coarse particles. This phenomenon, which leads to TaC sedimentation in the bottom of the ingot, because of their high volume mass (almost the double of the liquid one) and the electromagnetic stirring, is also met for the {10 wt.% Al} – containing alloy which is itself consequently almost free of TaC carbides in the core of the ingot. However, curiously, this does not seem threatening its oxidation and creep behaviors which appeared rather interesting, as evidenced by the two tests performed on this alloy in this study.

It remains, nevertheless, that these losses in TaC must be limited or suppressed, since the alloys containing 10 wt.% Al (certainly more oxidation resistant than the ones with only 5 wt.% Al), does not receive benefit from the expensive element Ta introduced in the charge before fusion. Remembering the very dense (too dense?) network of eutectic TaC seen in the Co5 alloy, one can think to decrease the contents in Ta and C (to 3 or 1.5 wt.% Ta and 0.2 or 0.1 wt.% C) to avoid pre–eutectic TaC formation.

Another solution can be achieving the isothermal chemical homogenization in liquid state (prior to solidification) at a temperature higher than the one made here, and by ac celerating the cooling in order to have much less time for the eventual pre–eutectic TaC to move downwards and to allow the growing dendritic matrix catching them.

References

[1] C.T. Sims, W.C. Hagel, (1972) The Superalloys. John Wiley & Sons, New York.

[2] M.J. Donachie, S.J. Donachie, (2002) Superalloys: A technical guide (2nd Ed.). Materials Park: ASM International. [DOI]

[3] P. Berthod, S. Michon, L. Aranda, S. Mathieu, J.C. Gachon, (2003). Experimental and thermodynamic study of the microstructure evolution in cobalt-base superalloys at high temperature. Calphad, 27(4), 353-359. [DOI]

[4] S. Michon, P. Berthod, L. Aranda, C. Rapin, R. Podor, P. Steinmetz, (2003). Application of thermodynamic calculations to study high temperature behavior of TaC-strengthened Co-base superalloys. Calphad, 27(3), 289-294. [DOI]

[5] S. Michon, L. Aranda, P. Berthod, P. Steinmetz, (2004). High temperature evolution of the microstructure of a cast cobalt base superalloy-Consequences on its thermomechanical properties. Revue de Métallurgie, 101(9), 651-662. [DOI]

[6] W.V. Youdelis, O. Kwon, (1983). Carbide phases in cobalt base superalloy: role of nucleation entropy in refinement. Metal science, 17(8), 379-384. [DOI]

[7] M. Montazeri, F.M. Ghaini, A. Farnia, (2011). Cobalt-based superalloy. International Journal of Materials Research. (formerly Z. Metallkd.), 102, 12. [DOI]

[8] G.M. Janowski, R.W. Heckel, B. Pletka, (1986). The effects of tantalum on the microstructure of two polycrystalline nickel-base superalloys: B-1900+ Hf and MAR-M247. Metallurgical Transactions A, 17(11), 1891-1905. [DOI]

[9] S. Gao, J. Hou, F. Yang, Y. Guo, L. Zhou, (2017). Effect of Ta on microstructural evolution and mechanical properties of a solid-solution strengthening cast Ni-based alloy during long-term thermal exposure at 700° C. Journal of Alloys and Compounds, 729, 903-913. [DOI]

[10] P. Berthod, L. Aranda, C. Vébert, S. Michon, (2004). Experimental and thermodynamic study of the high temperature microstructure of tantalum containing nickel-based alloys. Calphad, 28(2), 159-166. [DOI]

[11] P. Berthod, (2022). As-Cast microstructures of high entropy alloys designed to be TaC-strengthened. Journal of Metallic Material Research, 5(2), 4685. [DOI]

[12] P. Berthod, (2023). Reaction with hot air of high entropy alloys strengthened by monocarbides formed from heavy metals: assessment of the oxidation kinetics from the analysis of the chemically changed subsurfaces. Bulletin of Scientific Research, 5(2), 9-17. [DOI]

[13] P. Kofstad, (1988). High temperature corrosion ((Book)). London and New York, Elsevier Applied Science, 1988, 568.

[14] D.J. Young, (2016) High Temperature Oxidation and Corrosion of Metals (2nd Ed.). Amsterdam: Elsevier. [DOI]

[15] P. Berthod, (2005). Kinetics of high temperature oxidation and chromia volatilization for a binary Ni–Cr alloy. Oxidation of Metals, 64(3), 235-252. [DOI]

Funding

No funding was received for the conduct of this research

Conflict of interest

The authors declare that no conflict of interest exists.

Does the Article Screened for Similarity?

Yes.

About the License